Journal of Molecular Graphics and Modelling 51 (2014) 128–136

Contents lists available at ScienceDirect

Journal of Molecular Graphics and Modelling

journal homepage: www.elsevier.com/locate/JMGM

Quantum chemical characterization of zwitterionic structures: Supramolecular complexes for modifying the wettability of oil–water–limestone system

Ernesto Lopez-Chavez[a,*], Alberto Garcia-Quiroz[a], Gerardo Gonzalez-Garcia[a], Gabriela E. Orozco-Duran[a,b], Luis S. Zamudio-Rivera[c], José M. Martinez-Magadan[c], Eduardo Buenrostro-Gonzalez[c], Raul Hernandez-Altamirano[c]

[a] Programa de Ingeniería Molecular y Nuevos Materiales de la Universidad Autónoma de la Ciudad de México, Academia de Física, Av. Fray Servando Teresa de Mier 92-110, Col. Centro Histórico, Delegación Cuauhtémoc, CP 06080 México, D.F., Mexico
[b] Escuela Superior de Física y Matemáticas del Instituto Politécnico Nacional, Edificio 9 de la Unidad Profesional Adolfo López Mateos, Col. Lindavista, Delegación Gustavo A. Madero, CP 07738 México, D.F., Mexico
[c] Instituto Mexicano del Petróleo, Eje Central Lázaro Cárdenas Norte 152, Col. San Bartolo Atepehuacan, CP 07730 México, D.F., Mexico

ARTICLE INFO

Article history:
Accepted 28 April 2014
Available online 6 May 2014

Keywords:
Oil recovery
Zwitterionic liquid
Reactivity
Selectivity
HOMO and LUMO orbitals

ABSTRACT

In this work, we present a quantum chemical study pertaining to some supramolecular complexes acting as wettability modifiers of oil–water–limestone system. The complexes studied are derived from zwitterionic liquids of the types N′-alkyl-bis, N-alquenil, N-cycloalkyl, N-amyl-bis-beta amino acid or salts acting as sparkling agents. We studied two molecules of zwitterionic liquids (ZL10 and ZL13), HOMO and LUMO levels, and the energy gap between them, were calculated, as well as the electron affinity (EA) and ionization potential (IP), chemical potential, chemical hardness, chemical electrophilicity index and selectivity descriptors such Fukui indices. In this work, electrochemical comparison was realized with cocamidopropyl betaine (CPB), which is a structure zwitterionic liquid type, nowadays widely applied in enhanced recovery processes.

1. Introduction

For over 30 years, chemically-based improved oil recovery methods have generated great interest among researchers and technologists [1,2]. Chemical methods focus mainly on alkaline–surfactant-polymer (ASP) processes that involve the injection of micellar-polymers into the reservoirs. Chemical flooding reduces the interfacial tension between in-place crude oil and injected water, allowing the oil to be extracted. Micellar fluids are composed largely of surfactants mixed with water. The twice-fold goal of polymer floods is to shut off excess water in the producing wells while improving the sweep efficiency in order to produce more oil. Chemical field trials by industry indicate that surfactants can recover up to an additional 28% of reservoir oil; however the economics have not been favorable when the price of oil is factored against the cost of surfactants and polymers [3]. A new chemical product, based on novel molecules of zwitterionic liquid (ZL), has recently been proposed as an oil recovery enhancer. A great amount of studies on the structural, physical and chemical properties of zwitterionic liquids [3] have been carried out over the last two decades [4]. The results of these studies show the beginning of a new, improved, oil recovery method [5,6]. In the beginning of the year 2010, two new structures, based on zwitterionic liquids (ZL10 and ZL13), were proposed by Zamudio-Rivera et al. [7,8], based on the consideration that germinal zwitterionic molecules are characterized by having two hydrocarbon chains, one bridge, and two polar groups of zwitterionic class. Since then, as far as we know, no other authors have proposed similar models [9].

Although a large variety of new ZL forms structures have been proposed, many of their physical and chemical properties have not yet been reported or clearly understood, so that a deeper study is undoubtedly necessary [10].

Among the important physicochemical properties of ZL structures, the reactivity and selectivity descriptors play a key role. The knowledge of both global and local reactivity descriptors of ZL structures will allow us to predict the wettability-modifying ability of these molecules on oil–limestone and water–limestone systems. Presumably, even a quick analysis of these values can be used to understand the relationships between the structure, the

* Corresponding author. Tel.: +52 55 51349804; fax: +52 55 55862957.
E-mail addresses: elopezc_h@hotmail.com (E. Lopez-Chavez), albertogaqa@hotmail.com (A. Garcia-Quiroz).

http://dx.doi.org/10.1016/j.jmgm.2014.04.013
1093-3263/

stability and the electrochemistry of this molecule. In addition, the understanding of the chemical mechanisms of reaction between ZL and other molecules will allow us to visualize their potential technological applications in enhanced oil recovery (EOR) methods.

One of the most important questions connected with the problem of reactivity of molecules in different environmental conditions is the prediction and interpretation of the preferred direction of a reaction and the product formation [11]. The study of molecular interactions has been a great challenge from the experimental and theoretical point of view [12]. There have been a lot of attempts to explain the nature of bonding and reactivity of molecular systems based on some facts and intuitive ideas [13,14]. During quantum chemical methods development, many of the empirical chemical concepts were rigorously derived, thus providing a method for the calculation of chemical properties based on molecular structure and properties [15].

Within the context of density functional theory (DFT), rigorous theoretical basis for the descriptors of global and local reactivity indices have been provided. These reactivity indices are better appreciated in terms of the associated electronic structure principles such as electronegativity equalization principle, hard–soft acid–base (HSAB) principle [16], maximum hardness principle (MHP) [17], minimum polarizability principle (MPP) [18] and generalized philicity [19]. The global reactivity indices such as chemical hardness, chemical potential and electrophilicity are used to understand the chemical reactivity; whereas the local quantities such Fukui functions, local softness and local philicity indices have been employed to prove site selectivity and the reactivity of molecular systems of size ranging from small organic molecules to reasonably large drug molecules [20,21].

Furthermore, in Fukui's Frontier Orbital Theory [22], Fukui functions measure how sensitive a molecule's chemical potential is for external perturbations at a particular point, i.e., chemical reactivity toward nucleophiles or electrophiles is interpreted in terms of the highest occupied molecular orbital (HOMO) or lowest unoccupied molecular orbital (LUMO) electron density. For an electrophilic attack, the reaction will have effect where the HOMO electron density is the largest in the molecule. Similarly, for a nucleophilic reaction, the LUMO electron density indicates the chosen sites in the molecule. Fukui functions have been calculated for a large group of organic molecules, and it was thought that their values should always be positive, however, the occurrence of negative Fukui functions has been demonstrated by means of the electronegativity equalization method [23].

In this work, based on the above-mentioned issues, we have calculated chemical reactivity and selectivity indices of the most stable structures of ZL10 and ZL13 molecules with the aim of predicting the ability of molecules to undergo addition reactions and finding the preferred directions and sites of reaction on oil (asphaltene), rock (calcite or limestone) and water.

2. Methods

Since we treat the ZL10 and ZL13 as isolated molecules, the methodology used in this work is based on calculations performed with DMol3, a DFT computational code [24] of Materials Studio 6.0 specialized in quantum mechanical calculations on molecules.

The geometry of ZL10 and ZL13 are depicted in Figs. 1 and 2, respectively, along with atom numbering of both carbon and hydrogen atoms, which will be resumed in Tables 2 and 3 as charge distribution data on the respective structures. The geometries of these structures were optimized using the functional LDA-VWN [24] with a DN basis set. Previous studies on similar molecular systems show that LDA-VWN provides comparatively reliable results [25]. The calculations were carried out using DFT effective core potential as approximation of treatment of core electrons, multipolar expansion hexadecapole, smearing 0.005 Ha, direct inversion in an iterative (DIIS size = 10) subspace was used to speed up SCF convergence.

To study reactivity and selectivity of ZL10 and ZL13 based on DFT, the following reactivity and selectivity descriptors were calculated for minimum energy structure: the ionization potential (IP) and electron affinity (EA) through [26]

$$\mathrm{IP} = E(M^+) - E(M) \tag{1}$$

$$\mathrm{EA} = E(M) - E(M^-) \tag{2}$$

where $E(M^+)$ and $E(M^-)$ are the total energies of the ionic state of each molecule M; i.e., IP and EA are the vertical ionization potential and vertical well of the neutral, respectively.

The chemical potential μ and hardness η are used extensively to make predictions about chemical behavior. The chemical potential μ is defined as the first derivative of the total energy respect to the number of electrons. The hardness is defined as the second derivative of the total energy, together with the concept of electronegativity and the principle of equalization of electronegativities, has been used to develop the principle of hard and soft acids and bases. The finite difference approximation applied to the chemical potential μ and hardness η leads to

$$\mu = -\frac{\mathrm{IP} + \mathrm{EA}}{2} \tag{3}$$

and

$$\eta = \frac{\mathrm{IP} - \mathrm{EA}}{2} \tag{4}$$

electrophilicity index (ω) is obtained with next equation:

$$\omega = \frac{\mu^2}{2\eta} \tag{5}$$

From there, Mulliken [27] population scheme is used in order to provide Fukui function (FF) values, charge distribution on each atom [28] of ZL10 and ZL13. For a system of N electrons, independent calculations have been made using Mulliken scheme in $N-1$, N and $N+1$, electronic systems with the same molecular geometry to get the charges $q_k(N-1)$, $q_k(N)$ and $q_k(N+1)$ for all atoms k and these values were substituted in the next equations:

$$f_k^+ = q_k(N+1) - q_k(N) \tag{6}$$

$$f_k^- = q_k(N) - q_k(N+1) \tag{7}$$

$$f_k^0 = \frac{q_k(N+1) - q_k(N-1)}{2} \tag{8}$$

which represent nucleophilic, electrophilic and radical attack, respectively.

3. Results and discussion

3.1. Geometry and stability

The minimum energy of ZL10 and ZL13 structures, are shown in Figs. 1 and 2, respectively, and they are constituted by polyglycols derived from ethylene oxide and propylene oxide, in conjunction with two hydroxyl groups, alkyl amines, acrylic acid. ZL10 has each alkyl chain with just 10 carbon atoms, while the ZL13 has 13 carbon atoms in each alkyl chain. This result is consistent with the general structure of germinal zwitterionic liquid reported by Yoshizawa [29].

In this work, the total energy of ZL10 and ZL13 structures refers to the sum of energy components (atomic energies, kinetic energy, electrostatic energy, exchange-correlation energy, spin polarization energy, and DFT-D correction) of a specific arrangement of atoms corresponding to ground state molecule structure. The zero

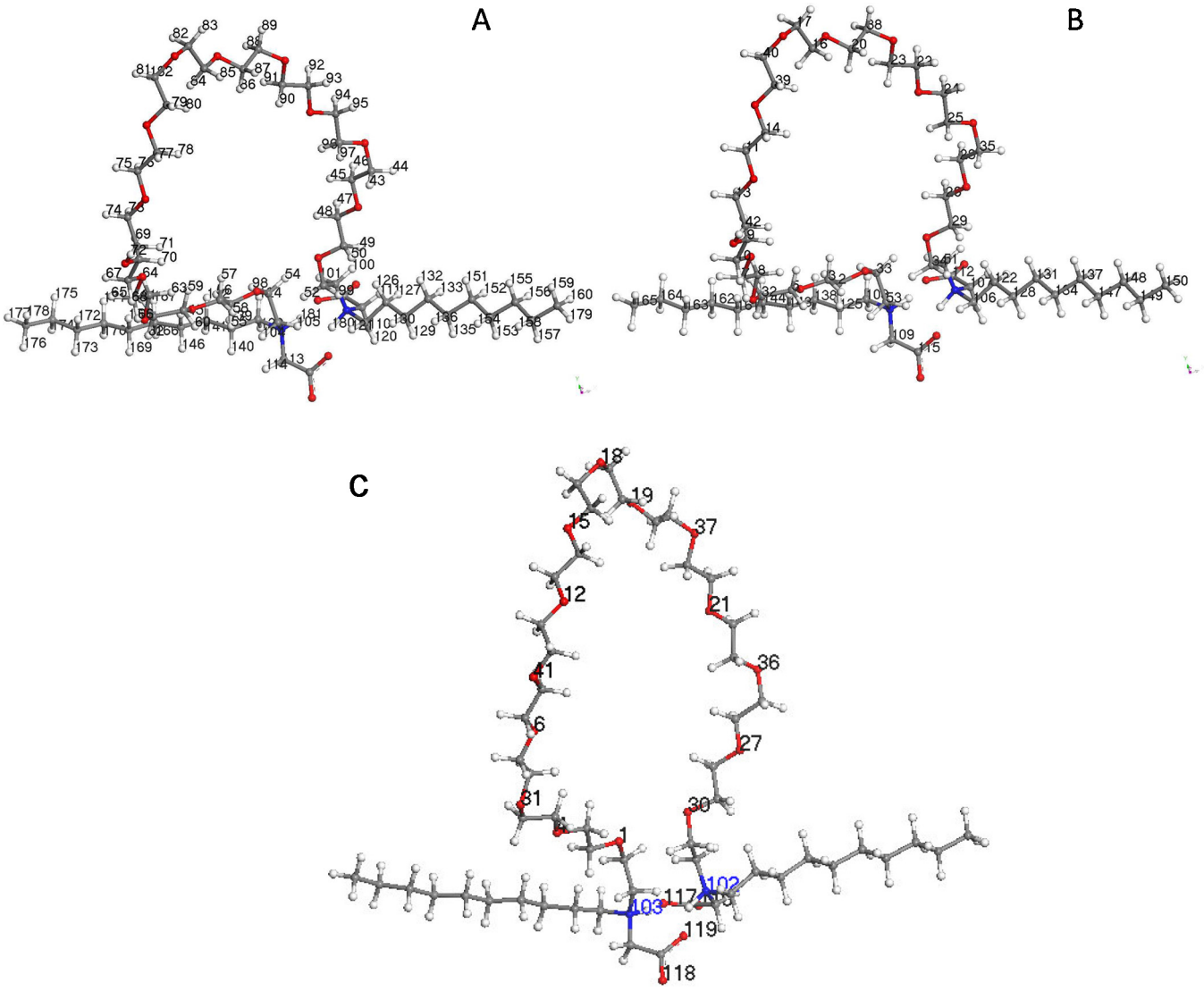

Fig. 1. ZL10 zwitterionic liquid minimized energy structure showing the number of the different types of atoms. (A) Hydrogen atoms, (B) carbon atoms and (C) oxygen and nitrogen atoms.

energy is taken to be the infinite separation of all electrons and nuclei, so the total energy is generally negative, corresponding to a bound state. This quantity should not be confused with the binding energy. The binding energy reported in DMol3 is the one used to dissociate the molecules into atoms at infinite separations.

Both of these quantities were calculated using DFT theory as it is implemented in the software package DMol3 of Materials Studio [24].

The components of ZL structure are mainly the next: a polyglycol chain, located in the central part of the ZL structures; two alkyl amines having an alkyl chain each, located at the ends of polyglycols; four-H radical type; and two pairs of oxygen atoms at the ends of the ZL structures.

The binding, or cohesive, energy is seen to be −20,418.872 kcal/mol (−885.25 eV) for ZL10 and −22,474.501 kcal/mol (−974.567 eV) for ZL13, which is an indicative of having a good relative stability of both structures. But, this result indicates that ZL13 is more stable than ZL10, since ZL13 requires more energy to be separated into its individual atoms; disassemble.

The total energy for ZL10 and ZL13 structures are found to be −2,231,871.876 kcal/mol (−96,783.65 eV) and −2,378,641.373 kcal/mol (−103,145.63 eV), respectively. The DFT total energy ingredients for ZL10 and ZL13 are given in Table 1.

Table 1
Total energy components for each ZL10 and ZL13 structure.

Energy components	ZL0	ZL13
Sum of atomic energies [eV]	−95,898.23	−102,170.36
Kinetic energy [eV]	−1336.17	−1459.81
Electrostatic energy [eV]	−66.34	−79.60
Exchange-correlation energy [eV]	286.57	314.71
Spin polarization energy [eV]	249.73	273.40
DFT-D correction energy [eV]	−19.23	−23.95
Total energy [eV]	−96,783.65	−103,145.63

It is important to observe when contributions from all energy components are added, except sum of atomic energies, the result is equal to binding energy. The sum of atomic energies is the major contribution to the total energy, while negative kinetic energy is the major contributor to binding energy.

The average bond lengths in the different regions of ZL10 are distributed in the following way: in alkyl chain of alkyl amine, C—C bond length is ranged from 1.503 Å to 1.527 Å, while C—H bond length ranged from 1.097 Å to 1.112 Å, N—C bond length is ranged

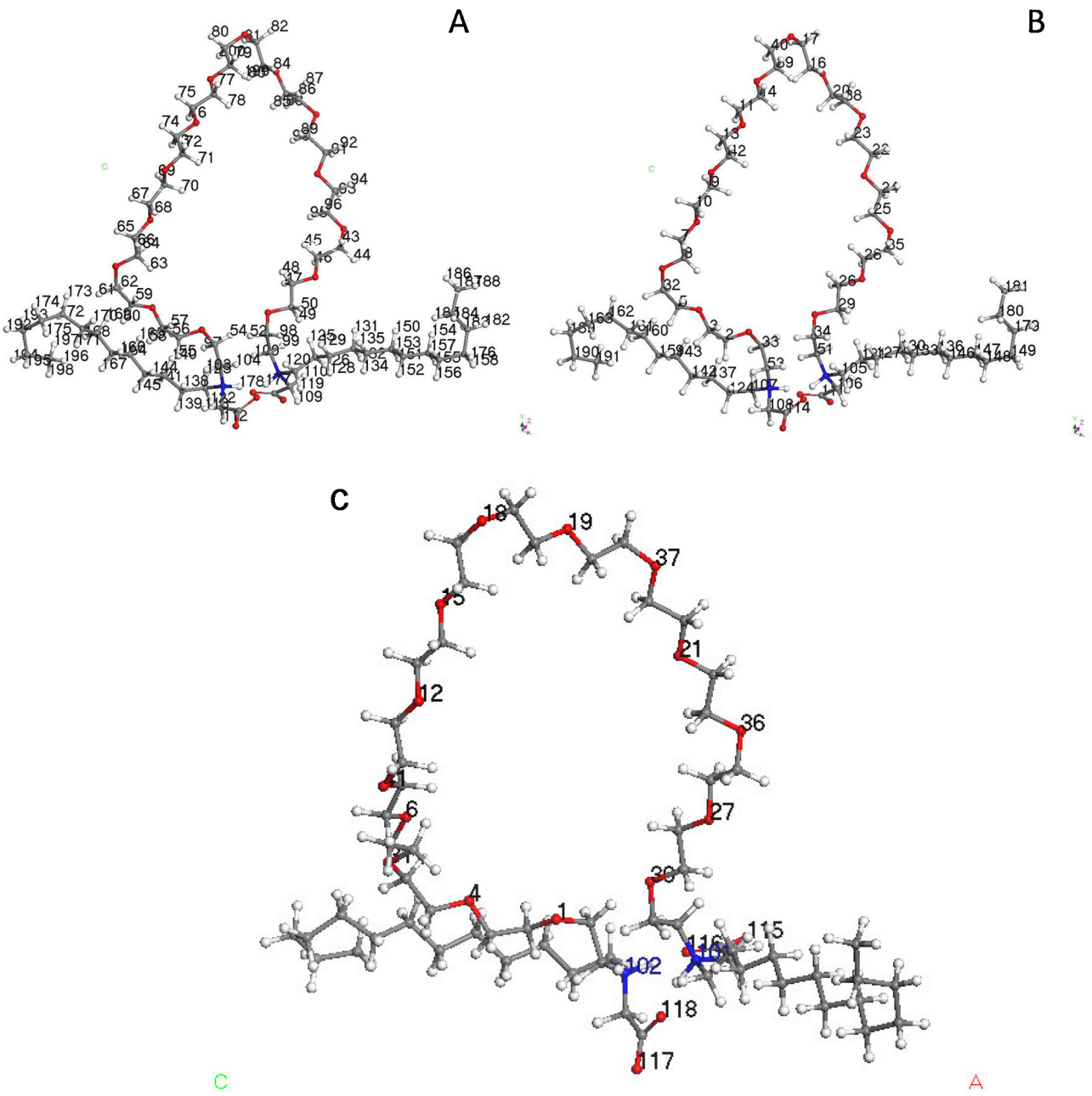

Fig. 2. ZL13 zwitterionic liquid minimized energy structure showing the number of the different types of atoms. (A) Hydrogen atoms, (B) carbon atoms and (C) oxygen and nitrogen atoms.

from 1.488 Å to 1.502 Å. Besides, C—O bond length, in polyglycol, range from 1.440 Å to 1.456 Å. In both extreme ZL10 ends, C—O bond length is 1.303 Å for one bond and 1.260 Å for the other. Finally, in radical zones, C—H bond length range from 1.096 Å to 1.112 Å.

For ZL13, C—C bond length, in alkyl chain of alkyl amine, is in the range 1.509 Å–1.522 Å, C—H bond length from 1.110 Å to 1.112 Å, N—C bond length from 1.467 Å to 1.498 Å. In polyglycol, C—O bond length is ranged from 1.449 Å to 1.458 Å. C—O bond length, in the extreme ZL13 ends, is 1.312 Å for one bond and 1.315 Å for the other. In radical zones, C—H bond length is from 1.089 Å to 1.120 Å.

All bond lengths, in both ZL structures, are within the values reported for other structures [30].

3.2. Mulliken electron populations

Mulliken population analysis is a very effective method for predicting sites susceptible to nucleophilic or electrophilic attack and other aspects of molecular interaction.

In this work, Mulliken charge population were used in order to find the nature of supramolecular interactions between ZL (ZL10 and ZL13), behaving as a host, with other molecules, such as crude oil or asphaltenes (as guest), to produce a complex "host–guest "or supermolecular system. In this context, if we regard supramolecular interactions in their simplest sense, as involving some type of binding (no-covalent), we must determine what it is doing the binding. In this study, the host (ZL10 or ZL13) is defined as the molecular entity possessing convergent binding sites. The guest (for example, asphaltene molecules) possesses divergent binding sites [31]. Then supramolecular complexes are composed of two or more molecules or ions hold together by different types of interactions.

Table 2
Charge distribution on atoms of ZL10.

Hydrogen (num)	Charge	Hydrogen (num)	Charge	Hydrogen (num)	Charge	Carbon (num)	Charge	Carbon (num)	Charge
43	0.156	82	0.157	136	0.12	5	−0.049	131	−0.236
44	0.167	83	0.166	139	0.102	7	−0.032	134	−0.23
45	0.157	84	0.166	140	0.166	8	−0.06	137	−0.233
46	0.154	85	0.157	141	0.136	9	−0.059	138	−0.24
47	0.157	86	0.155	142	0.133	10	−0.029	143	−0.236
48	0.157	87	0.157	145	0.126	11	−0.03	144	−0.231
49	0.184	88	0.155	146	0.123	13	−0.047	147	−0.227
50	0.166	89	0.165	151	0.116	14	−0.041	148	−0.227
52	0.188	90	0.159	152	0.116	16	−0.068	149	−0.234
54	0.189	91	0.157	153	0.116	17	−0.045	150	−0.366
55	0.186	92	0.151	154	0.115	20	−0.055	161	−0.234
56	0.18	93	0.152	155	0.113	22	−0.03	162	−0.228
57	0.16	94	0.151	156	0.115	23	−0.059	163	−0.231
58	0.158	95	0.15	157	0.117	24	−0.03	164	−0.232
59	0.153	96	0.161	158	0.118	25	−0.052	165	−0.374
60	0.153	97	0.152	159	0.121	26	−0.04	**Oxygen (num)**	**Charge**
61	0.154	98	0.186	160	0.121	28	−0.054	1	−0.483
62	0.169	99	0.177	166	0.121	29	−0.068	4	−0.527
63	0.163	100	0.192	167	0.116	32	−0.051	6	−0.533
64	0.156	101	0.213	168	0.118	33	−0.12	12	−0.532
65	0.151	104	0.195	169	0.117	34	−0.113	15	−0.531
66	0.152	105	0.197	170	0.118	35	−0.053	18	−0.516
67	0.152	110	0.21	171	0.116	38	−0.054	19	−0.527
68	0.147	111	0.198	172	0.114	39	−0.03	21	−0.535
69	0.164	113	0.211	173	0.118	40	−0.083	27	−0.525
70	0.155	114	0.217	174	0.117	42	−0.061	30	−0.499
71	0.153	120	0.189	175	0.119	51	−0.18	31	−0.523
72	0.167	121	0.191	176	0.123	53	−0.171	36	−0.526
73	0.153	123	0.189	177	0.121	106	−0.155	37	−0.52
74	0.152	124	0.193	178	0.122	107	−0.182	41	−0.519
75	0.148	126	0.124	179	0.119	108	−0.153	116	−0.572
76	0.153	127	0.165	180	0.408	109	−0.188	117	−0.599
77	0.152	129	0.136	181	0.386	112	0.43	118	−0.572
78	0.155	130	0.134	182	0.159	115	0.432	119	−0.591
79	0.148	132	0.124	**Carbon (num)**	**Charge**	122	−0.274	**Nitrogen (num)**	**Charge**
80	0.147	133	0.124	2	−0.068	125	−0.274	102	−0.533
81	0.165	135	0.119	3	−0.04	128	−0.236	103	−0.508

Table 2 shows the charge distribution of hydrogen-, carbon-, oxygen- and nitrogen-atoms, which are shown and numbered in Fig. 1a–c, respectively, of a ZL10 molecule. The analysis of such table shows the formation of electric dipoles between charges located on paired-atoms as: H155–C34; H59–C108, H60–C108, H71–C108, H73–C108, H76–C108; H70–C106, H78–C106, H86–C106, H88–C106; H56–C51; H52–C109, with electric dipolar moment, 5.47 dB; 5.93 dB, 5.78 dB, 12.2 dB, 12.1 dB, 12.9 dB, 10.9 dB, 13.3 dB, 12.1 dB, 12.6 dB, 5.05 dB, 4.18 dB, respectively. We can also observe that sites with higher concentration of negative charge are located on O115, O116, O117, and O118 oxygen atoms, which have charge equal to −0.542*e*, −0.585*e*, −0.547*e*, −0.576*e*, respectively. These atoms are located at the end of ZL10. Moreover, sites with higher concentration of positive charge are on H110, H111, H113, H114, H180, H181 hydrogen atoms, which are located on alkyl chains, and very close to N102, N103 nitrogen atoms. The charges of these atoms are 0.210*e*, 0.198*e*, 0.217*e*, 0.211*e*, 0.408*e*, 0.386*e*, respectively, where *e* is the absolute value of electron charge from now on.

It is also important to emphasize that H180 and H181 hydrogen atoms are bonded to electronegative N102 and N103 nitrogen atoms, respectively and met all the conditions to form interactions type hydrogen bonding with electronegative atoms of other molecules such as asphaltenes.

From the above analysis, we can say that ZL10 may form supramolecular interactions type ion–ion, ion–dipole, dipole–dipole and hydrogen bonds with other molecules as asphaltenes. Then ZL10 interacts with calcite rock surface system, because the wettability of calcite–water–oil system is modified.

On the other hand, for ZL13, Mulliken charge distribution on hydrogen-, carbon-, oxygen- and nitrogen-atoms is presented in Table 3. The atoms of ZL13 are presented and numbered in Fig. 2a–c, respectively. Similarly to ZL10 analysis, the formation of electric dipoles were found between charges localized on paired-atoms as: H132–C33; H150–C33, H169–C33, H186–C33, H188–C33; H43–C107; H46–C107, H76–C107; H85–C107, H96–C107; H86–C53; H89–C53; H88–C105, with electric dipolar moment, 5.16 dB; 6.54 dB, 3.87 dB, 9.19 dB, 9.9 dB, 8.93 dB, 7.50 dB, 12.2 dB, 12.9 dB, 9.56 dB, 12.8 dB, 11.2 dB, 12.8 dB, respectively.

In Tables 2 and 3 are showed that the partitioning behavior of the electron density for ZL13 atoms is very similar to the one for ZL10 atoms, since the sites with highest concentration of negative charge are located on O115, O116, O117 and O118 oxygen atoms, whose charge is equal to −0.542*e*, −0.585*e*, −0.408*e*, −0.576*e*, respectively. Moreover, these oxygen atoms are located at the end part of ZL13.

Furthermore, ZL13 sites with higher positive charge concentration are located on H109, H110, H112, H113, H177, H178 hydrogen atoms, which are located on the alkyl chains of the ZL13 structure, and very close to N101 and N102 nitrogen atoms. The charge of these hydrogen atoms is 0.217*e*, 0.213*e*, 0.218*e*, 0.214*e*, 0.392*e*, 0.404*e*, respectively.

Finally, we noted that covalent bonds, N101–H177 and N102–H178, meet the sufficient conditions to form bonds of the type of hydrogen bondings with other molecules.

So, these lead us to verify that both ZL10 and ZL13 may form supramolecular structures with other molecules through interactions such as: ion–ion, ion–dipole, dipole–dipole, and hydrogen bonds, mainly, since they are capable to modify the calcite–water–oil system wettability.

Table 3
Charge distribution on atoms of ZL13.

Hydrogen (num)	Charge	Hydrogen (num)	Charge	Hydrogen (num)	Charge	Carbon (num)	Charge	Carbon (num)	Charge
43	0.156	86	0.157	152	0.119	2	−0.116	136	−0.238
44	0.169	87	0.169	153	0.119	3	−0.082	137	−0.262
45	0.155	88	0.159	154	0.132	5	−0.1	142	−0.264
46	0.156	89	0.157	155	0.112	7	−0.031	143	−0.254
47	0.158	90	0.152	156	0.116	8	−0.05	146	−0.237
48	0.161	91	0.15	157	0.124	9	−0.06	147	−0.235
49	0.184	92	0.155	158	0.115	10	−0.033	148	−0.256
50	0.179	93	0.153	164	0.132	11	−0.039	149	−0.225
52	0.19	94	0.151	165	0.13	13	−0.046	159	−0.275
54	0.186	95	0.166	166	0.162	14	−0.037	160	−0.264
55	0.151	96	0.156	167	0.134	16	−0.074	161	−0.261
56	0.207	97	0.18	168	0.135	17	−0.043	162	−0.247
57	0.168	98	0.182	169	0.122	20	−0.051	163	−0.266
58	0.167	99	0.195	170	0.139	22	−0.031	179	−0.243
59	0.166	100	0.195	171	0.146	23	−0.051	180	−0.235
60	0.155	103	0.209	172	0.134	24	−0.034	181	−0.372
61	0.151	104	0.196	173	0.158	25	−0.064	189	−0.232
62	0.171	109	0.217	174	0.125	26	−0.036	190	−0.226
63	0.158	110	0.213	175	0.121	28	−0.056	191	−0.402
64	0.154	112	0.218	176	0.114	29	−0.069	**Oxygen (num)**	**Charge**
65	0.155	113	0.214	177	0.392	32	−0.072	1	−0.485
66	0.151	119	0.196	178	0.404	33	−0.122	4	−0.476
67	0.151	120	0.193	182	0.112	34	−0.117	6	−0.533
68	0.153	122	0.2	183	0.128	35	−0.052	12	−0.533
69	0.166	123	0.193	184	0.118	38	−0.056	15	−0.535
70	0.155	125	0.112	185	0.132	39	−0.023	18	−0.512
71	0.154	126	0.162	186	0.122	40	−0.095	19	−0.528
72	0.166	128	0.131	187	0.121	42	−0.053	21	−0.536
73	0.153	129	0.137	188	0.122	51	−0.163	27	−0.532
74	0.151	131	0.126	192	0.116	53	−0.157	30	−0.491
75	0.152	132	0.122	193	0.118	105	−0.159	31	−0.512
76	0.156	134	0.123	194	0.12	106	−0.188	36	−0.521
77	0.153	135	0.119	195	0.116	107	−0.156	37	−0.524
78	0.154	138	0.171	196	0.143	108	−0.188	41	−0.522
79	0.15	139	0.165	197	0.136	111	0.445	115	−0.542
80	0.165	140	0.131	198	0.124	114	0.434	116	−0.585
81	0.158	141	0.149	199	0.144	121	−0.271	117	−0.547
82	0.168	144	0.145	200	0.164	124	−0.287	118	−0.576
83	0.164	145	0.137			127	−0.237	**Nitrogen (num)**	**Charge**
84	0.161	150	0.122			130	−0.239	101	−0.533
85	0.156	151	0.116			133	−0.231	102	−0.537

3.3. ZL10 and ZL13 electrochemistry

In order to analyze the reactive nature of these zwitterionic liquid molecules (ZL10 and ZL13) and to make an electrochemical comparison with other zwitterionic liquids surfactants, some global reactivity descriptors were calculated.

In this work, the electrochemical comparison was realized with a cocamidopropyl betaine (CPB), which is also a zwitterionic liquid structure type (see Fig. 3), widely applied in enhanced recovery processes.

The ZL structures electrochemistry was discussed by comparing the energy associated with the HOMO and LUMO orbitals for each molecule. The electron affinity (EA) and the ionization potential (IP) to that for CPB was obtained. See Table 4 where the values of these properties are presented; EA and IP descriptors.

The ZL10 molecule exhibits a 4.743 eV energy gap, the ZL13 presents a 4.858 eV energy gap, while CPB had a 4.831 eV energy gap. In general, the larger the energy gap between the frontier orbitals, the greater the difficulty of transferring electrons from HOMO to LUMO orbitals, while increasing the energy gap then the inactivity also increases. Thus, according to this criterion, ZL10 is much less stable than CPB and, in turn, CPB is much less stable than ZL13.

Moreover, according to IP values, shown in Table 4, the ZL13 molecule requires major energy to release an electron, from its structure to infinity, than CPB. The same is for CPB that needs more energy to do so than ZL10. In this sense, it is found that the minimum energy required to release an electron from ZL13, which it is 7.2481 eV, is greater than the one required to release an electron from CPB molecule, which it is 7.1372 eV and is also greater than the one needed to the same for ZL10 molecule which needs 7.0205 eV of energy.

Furthermore, Table 4 data indicates that the ZL13 maximum energy released, is 1.2948 eV, when it accepts an electron to form a radical-anion. This energy is greater than the one released by CPB molecule and also greater than the energy liberated by ZL10 molecule for accepting an electron, that is, 1.2397 eV and 1.2145 eV, respectively. The EA of the three structures are positive, which indicates that an electron always will be bounded to the molecules; the ZL13 EA's is larger than the one CPB and larger to the one of ZL10. So, ZL13 has greater tendency to reject electrons than CPB molecule, in turn, than ZL10.

Our results suggest that ZL13 is the structure most inactive than CPB and ZL10 molecules. Moreover, these results proved that ZL10 is the most reactive structure comparing to CPB and ZL13 molecules. Meaning that ZL13 is more stable than CPB, in turn, than ZL10.

3.4. Reactivity and selectivity

Global reactivity indexes are calculated in very efficient and robust way in the framework of density functional theory, DFT. In order to perform a comparison of reactivity and selectivity between

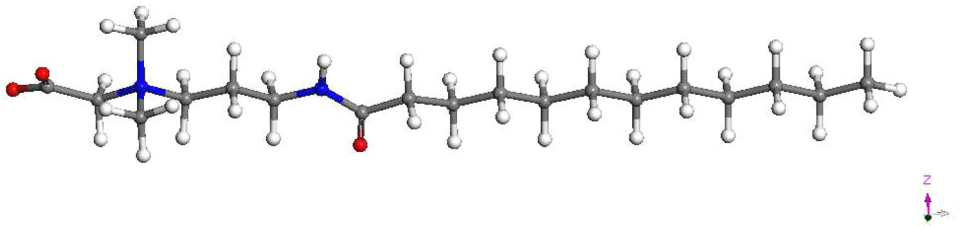

Fig. 3. Cocamidopropyl betaine (CPB) minimized energy structure.

Table 4
Energies of HOMO, LUMO, and ΔE gap; estimated electron affinities (EA), ionization potentials (IP) and reactivity global indicators (μ, η and ω)* for ZL10, ZL13 and cocamidopropyl betaine.

	HOMO (eV)	LUMO (eV)	ΔE (eV)	EA (eV)	IP (eV)	μ (eV)	η (eV)	ω (eV)
ZL10	−5.859	−1.116	4.743	1.2145	7.0205	−4.1175	5.8060	1.4600
ZL13	−5.958	−1.100	4.858	1.2984	7.2481	−4.2733	5.9497	1.5346
Cocamidopropyl betaine	−5.379	−0.548	4.831	1.2397	7.1372	−4.1885	5.8975	1.4873

Chemical potential – μ, and hardness – η, and electrophilicity index – ω.

the ZL's structures (ZL10 and ZL13) and cocamidopropyl betaine (CPB), we calculated the reactivity global indicators (μ, η and ω). The chemical potential values, hardness and electrophilicity index are shown in Table 4.

The η column, in Table 4, showed that the ZL13 has the highest hardness value compared to every other hardness value calculated. This means that ZL13 is the most resistant electronic structure for modifications. This result is consistent with the Pearson principle

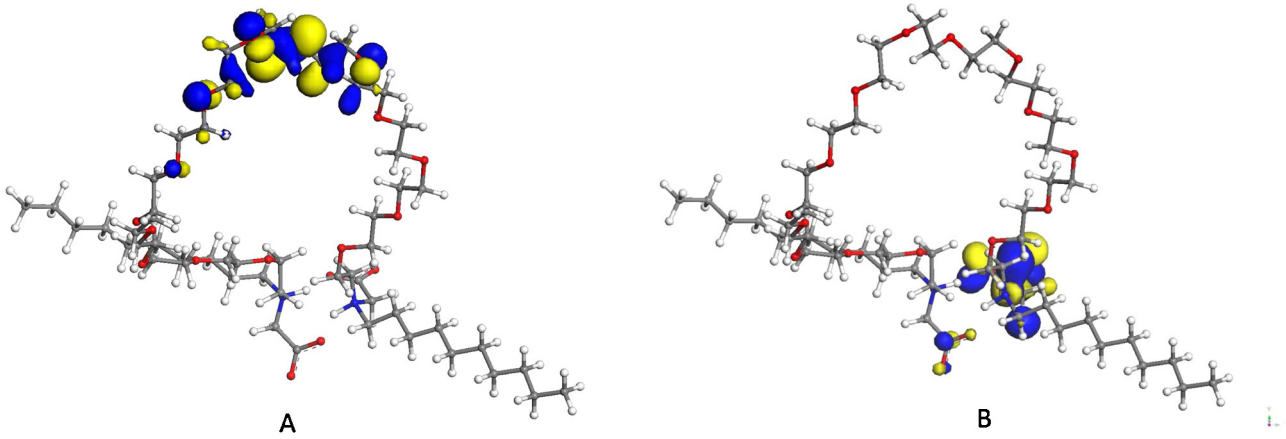

Fig. 4. HOMO and LUMO orbital shapes and sizes for the ZL10. (A) HOMO orbital, and (B) LUMO orbital.

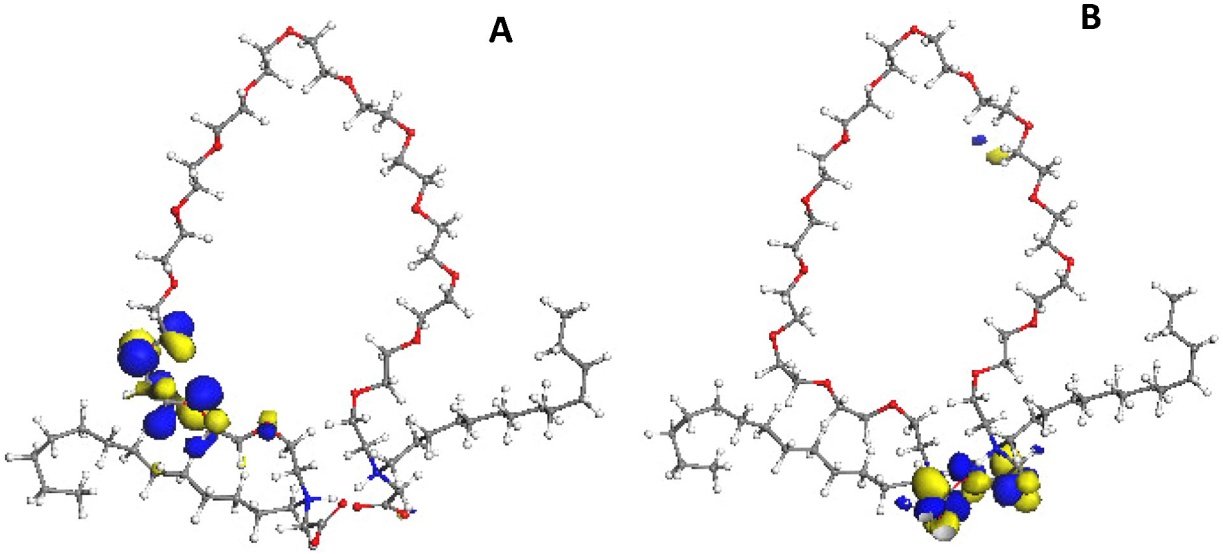

Fig. 5. HOMO and LUMO orbital shapes and sizes for the ZL13. (A) HOMO orbital, and (B) LUMO orbital.

of maximum hardness, whereby the more stable chemical species tend to maximum hardness.

In addition, the ZL10 complex has the highest escaping tendency of electrons, since its chemical potential ($\mu = -4.1175$ eV) is the highest one obtained for all studied structures; which were $\mu = -4.1885$ eV for CPB and $\mu = -4.2733$ eV for ZL13. This implies that ZL13 has the greatest electronic cloud transfer and has the structure with more energy dropping when any infinitesimal electron charge amount enters to it.

Electrophilicity indexes confirmed a marked tendency, through chemical hardness values behavior, that a ZL10 molecule has the major capacity to exchange electrons with other substances. Since the electrophilicity indexes for ZL13 is greater than for CPB and greater than for ZL10. This is in a good agreement with the results obtained for EA, IP and for HOMO–LUMO gap. Thus, ZL13 is the molecule with greater stability with less electronic activity.

The ZL10 HOMO and LUMO orbitals are plotted in Fig. 4. The forms of these frontier orbitals illustrate the molecule type bonds, these are π bonds. The LUMO size showed an improved potential for accommodating excess electron charge around of an alkyl-amine zone, Fig. 4b; the form, the size and the calculated energy of LUMO indicate that ZL10 is a structure highly reactive in the alkyl-amine zone, since it receives electrons in this zone, mainly.

The ZL10 HOMO is depicted in Fig. 4a. The shape of this frontier orbital shows that in the polyglycol zone of the molecule the bonds are π-bonds predominantly. In this zone, the orbital presents many nodes, so that the molecule has few contributions of bonding character, predominating of antibonding characters. The rest of the molecule presents major stability and less reactivity.

Fig. 5 shows ZL13 HOMO and LUMO orbitals. The HOMO orbital is shown in Fig. 5a, where we can appreciate that it is localized in the extreme of the polyglycol zone, while the LUMO orbital is localized in zone of acrylic acids, Fig. 5b. These zones are those of maximum reactivity in the molecule.

3.5. ZL10 and ZL13 sites of reaction

It is possible to identify the active sites of the molecule in the study through local indicators of reactivity. This work uses the Fukui function as local indicator representing the sensitivity of the chemical potential for external perturbations.

Basically, the electron density change is measured while the electron number increases. Fukui functions are advocated as reactivity descriptors in order to identify the most reactive sites for electrophilic or nucleophilic reactions with other molecules.

For ZL10, the nucleophilic values (f^+), of Fukui functions, were obtained based on an active electron number of 590.1. They ranged values from −0.019 for C107 (see Fig. 1b) to 0.177 for O116 (see Fig. 1c). The electrophilic values (f^-), of Fukui functions, ranged from −0.013 for C20 (see Fig. 1b) to 0.06 for O116, as calculated by using an active electron number of 589.9. Finally, radical value (f^0) Fukui functions oscillated from −0.01 for C107 (see Fig. 1b) to 0.118 for O116 (see Fig. 1c). These results indicate that ZL10 reactivity is realized on sites C107, O116 and C20 (see Fig. 1).

Similarly, for ZL13, our calculations showed that nucleophilic, electrophilic and radical attacks are produced, principally, in sites O117 ($f^+ = 0.154$), O31 ($f^- = 0.16$), and O115 ($f^0 = 0.124$) (see Fig. 2c), respectively.

4. Conclusions

Theoretical studies, based on density functional theory, provided valuable information on the geometry, the stability, the electrochemistry, the reactivity and the selectivity of the ZL10 and ZL13 zwitterionic molecules.

ZL10 and ZL13 structures geometry optimizations were realized, and the structural and chemical stability of these molecules has been proved.

Mulliken population analyses indicated that ZL10 and ZL13 can form supramolecular structures with other molecules through: ion–ion, ion–dipole, dipole–dipole, and hydrogen bonds, interactions, mainly.

While ZL10 and ZL13 interact with calcite rock surface, the wettability of calcite–water–oil system is modified.

The binding energy values indicate that ZL13 is most stable than ZL10. The global reactivity indices, as well as the frontier orbital energy gaps, showed that ZL10 is the most reactive structure compared to the cocamidopropyl betaine, and to ZL13.

The ZL10 LUMO analysis showed a great potential for electron charge accommodation around the alkyl amine zone. Moreover, the ZL10 HOMO showed that, in polyglycols zone, the bonds are predominantly π-bonds. In this zone, the orbital presents many nodes, the molecule has few contributions of bonding character and the antibonding character is predominate.

ZL13 frontier orbital's indicated that HOMO orbital's is localized in the extreme polyglycol zone, while LUMO orbital's is localized in acrylic acids zone.

The ZL10 molecule maximum reactivity site is O116 and for ZL13 molecule the maximum reactivity sites are O117, O31 and O115.

All these results are very important in order to study the oil production processes and rock wettability change, by means of asphaltene–zwitterionic-liquid–water–calcite interactions.

Acknowledgments

We greatly acknowledge the financial support provided by the CONACYT-SENER-HIDROCARBUROS of Mexico under project no. 146735. Some authors also acknowledge to SECITI and UACM by 060/2013 agreement through PI2011-23R project. We also acknowledge to CONACyT – Mexico and to Sistema Nacional de Investigadores, SNI-CONACyT – Mexico. Also we greatly acknowledge to the Mexico City Autonomous University, UACM. The second author G-Q, A. also acknowledges Luisa Nabile Jeronimo Guerrero for her technical help at UACM.

References

[1] Vladimir Alvarado, Eduardo Manrique, Enhanced Oil Recovery: Field Planning and Development Strategies, Gulf Professional Publishing, Elsevier Burlington, Massachusetts, USA, 2010, ISBN 10: 1856178552/ ISBN 13: 9781856178556.
[2] L.W. Lake, Enhanced Oil Recovery, Prentice Hall, Englewood Cliffs, NJ, United States, 1989, ISBN: 0132816016/ 9780132816014.
[3] J.L. Sessler, P.A. Gale, W. Cho, Anion Receptor Chemistry, Royal Society of Chemistry, Cambridge, UK, 2006.
[4] J.M. Mahoney, A.M. Beatty, B.D. Smith, Selective recognition of an alkalihalide contact ion-pair, J. Am. Chem. Soc. 123 (2001) 5847–5848.
[5] L. Cosentino, Integrated Reservoir Management, IFP Publications, Editions Technip, Paris, France, 2001.
[6] J.J. Sheng, Modern Chemical Enhanced Oil Recovery: Theory and Practice, GGP Publications, Elsevier, San Francisco, USA, 2011.
[7] L.S. Zamudio-Rivera, US Patent 947, MX/E/2010/070416 (2010).
[8] L.S. Zamudio-Rivera, US Patent, US/2011/0138683A1 (2011).
[9] http://www.uspto.gov/patents/index.jsp
[10] P.G. Plieger, P.A. Tasker, S.G. Galbraith, Zwitterionic macrocyclic metal sulfate extractants containing 3-dialkylaminomethylsalicylaldimine units, Dalton Trans. 31 (2004) 3–31, 8.
[11] F.P. Schmidtchen, Tetazac – a novel artificial receptor for binding omega-amino carboxylates, J. Org. Chem. 51 (1986) 5161–5168.
[12] J.L. Sessler, A. Andrievsky, Sapphryin–lasalocid conjugate: a novel carrier for aromatic amino acid transport, Chem. Commun. (1996) 1119–1120.
[13] P. Debroy, M. Benerjee, M. Prasad, S.P. Moulik, S. Roy, Binding of amino acids into a novel multiresponsive ferrocene receptor having an one backbone, Org. Lett. 7 (2005) 403–406.
[14] R. Neubert, Ion-pair transport across membranes, Pharm. Res. 6 (1989) 743–747.
[15] D.A. Mazziotti, J. Chem. Phys. 121 (2004) 10957.
[16] R.G. Pearson, Hard and soft acids and bases – the evolution of a chemical concept, Coord. Chem. Rev. 100 (1990) 403–425.

[17] R.G. Parr, P.K. Chattaraj, Principle of maximum hardness, J. Am. Chem. Soc. 113 (1991) 1854–1855.
[18] P.K. Chattaraj, S. Sengupta, Popular electronic structure principles in a dynamical context, J. Phys. Chem. 100 (1996) 16126–16130.
[19] P.K. Chattaraj, B. Maiti, U. Sarkar, Philicity: a unified treatment of chemical reactivity and selectivity, J. Phys. Chem. A: Commun. 107 (2003) 4973–4975.
[20] P.K. Chattaraj, S. Nath, B. Maiti, Reactivity descriptors, in: J. Tollenaere, P. Bultinck, H.D Winter, W. Langenaeker (Eds.), Computational Medicinal Chemistry and Drug Discovery, Marcel Dekker, New York, 2003, pp. 295–322 (Chapter 11).
[21] R. Parthasarathi, J. Padmanabhan, U. Sarkar, B. Maiti, V. Subramanian, P.K. Chattaraj, Toxicity analysis of benzidine through chemical reactivity and selectivity profiles: a DFT approach, Int. Electron. J. Mol. Des. 2 (2003) 798–813.
[22] K. Fukui, T. Yonezawa, H. Shingu, A molecular orbital theory of reactivity in aromatic hydrocarbons, J. Chem. Phys. 20 (1952) 722.
[23] P. Bultinck, R. Carbó-Dorca, W. Langenaeker, Negative Fukui functions: new insights based on electronegativity equalization, J. Chem. Phys. 118 (10) (2003) 4349–4356.
[24] Material Studio v6.0.0, Accelrys, Inc., 10188 Telesis Court, Suite 100, San Diego, CA 92121, USA (www.accelrys.com), copyright (c) 2011.
[25] J.P. Perdew, J.A. Chevary, S.H. Vosko, K.A. Jackson, M.R. Pederson, D.J. Singh, C. Fiolhais, Atoms, molecules, solids, and surfaces: applications of the generalized gradient approximation for exchange and correlation, Phys. Rev. B 46 (1992) 6671–6687.
[26] J.P. Perdew, K. Burke, M. Ernzerhof, Generalized gradient approximation mode simple, Phys. Rev. Lett. 78 (1997) 1396.
[27] R.G. Parr, W. Yang, Density Functional Theory of Atoms and Molecules, Oxford University Press, Oxford, 1989.
[28] F.L. Hirshfeld, Bonded-atom fragments for describing molecular charge densities, Theor. Chim. Acta 44 (1997) 129–138.
[29] M. Yoshizawa, D.R. MacFarlane, M. Forsyth, H. Ohno, Zwitterionic liquid/acid mixtures as anhydrous proton conductivity systems, Electrochem. Soc. Proc. 24 (2004) 73.
[30] R.C. Weast, Handbook of Chemistry and Physics, 66th ed., CRC Press, Ohio, USA, 1985, ISBN: 0-8493-0465-2.
[31] J.D. Cram, M.J. Cram, Container Molecules and Their Guests Monographs in Supramolecular Chemistry, Published by Royal Society of Chemistry, Cambridge, Great Britain, 1997, ISBN 10: 9780851869728/ISBN 13: 0851869726.